Journal of Hazardous Materials 439 (2022) 129696

Contents lists available at ScienceDirect

Journal of Hazardous Materials

journal homepage: www.elsevier.com/locate/jhazmat

# Characterization of tars from recycling of PHA bioplastic and synthetic plastics using fast pyrolysis

Alican Akgül [a], Tania Palmeiro-Sanchez [b], Heiko Lange [c], Duarte Magalhaes [a,d], Sean Moore [e], Alexandre Paiva [f], Feyza Kazanç [a,*], Anna Trubetskaya [e,*]

[a] Mechanical Engineering Department, Middle East Technical University, Ankara, Turkey
[b] Department of Microbiology, National University of Ireland Galway, Galway, Ireland
[c] Department of Earth and Environmental Sciences, University of Milano-Bicocca, Piazza della Scienza 1, 20126 Milan, Italy
[d] Dept. of Energy, Environmental & Chemical Engineering, Washington University in St. Louis, St. Louis, MO 63130, USA
[e] Department of Engineering, University of Limerick, Castletroy, Ireland
[f] NOVA School of Science and Technology, Universidade NOVA de Lisboa, 2829-516 Caparica, Portugal

## HIGHLIGHTS

- Fast pyrolysis led to the conversion of **PHA** into value-added liquid compounds.
- Pyrolysis can potentially remove polymer matrices in the **CRFC** composites.
- Recovered **CRFC** carbon fibers retained length and position in a bundle after pyrolysis.
- The liquid fraction of block co-polymers comprise toxic and carcinogenic compounds.
- Fast pyrolysis of **PHA** and block co-polymers led to char yield of < 2wt. %.

## GRAPHICAL ABSTRACT

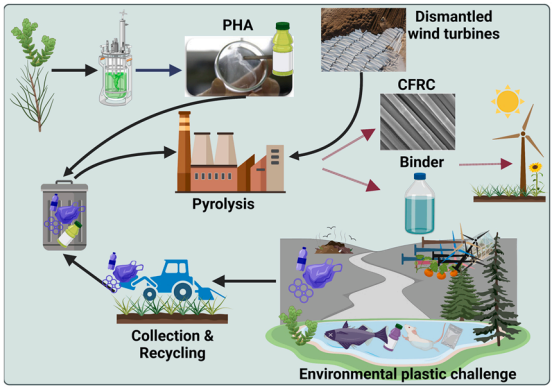


## ARTICLE INFO

Editor: R. Teresa

*Keywords:*
Polyhydroxyalkanoate (PHA)
Polyethylene terephthalate (PET)
Carbon fiber reinforced composites (CFRC)
Block co-polymers
Recycling
Fast pyrolysis

## ABSTRACT

The aim of this study was to investigate the pyrolysis products of polyhydroxyalkanoates (**PHAs**), polyethylene terephthalate (**PET**), carbon fiber reinforced composite (**CFRC**), and block co-polymers (**PS-b-P2VP** and **PS-b-P4VP**). The studied **PHA** samples were produced at temperatures of 15 and 50 °C (**PHA15** and **PHA50**), and commercially obtained from GlasPort Bio (**PHAc**). Initially, **PHA** samples were analyzed by nuclear magnetic resonance (NMR) spectroscopy and size exclusion chromatography (SEC) to determine the molecular weight, and structure of the polymers. Thermal techniques such as thermogravimetry (TG) and differential scanning calorimetry (DSC) analyses were performed for **PHA**, **CFRC**, and block co-polymers to investigate the degradation temperature range and thermal stability of samples. Fast pyrolysis (500 °C, ~$10^2$ °C $s^{-1}$) experiments were conducted for all samples in a wire mesh reactor to investigate tar products and char yields. The tar compositions were investigated by gas chromatography–mass spectrometry (GC–MS), and statistical modeling was performed.

* Corresponding authors.
*E-mail addresses:* fkazanc@metu.edu.tr (F. Kazanç), anna.trubetskaya@ul.ie (A. Trubetskaya).

https://doi.org/10.1016/j.jhazmat.2022.129696
Received 26 May 2022; Received in revised form 14 July 2022; Accepted 27 July 2022
Available online 28 July 2022

The char yields of block co-polymers and **PHA** samples (<2 wt. %) were unequivocally less than that of the **PET** sample (~10.7 wt. %). All **PHA** compounds contained a large fraction of ethyl cyclopropane carboxylate (~ 38–58 %), whereas **PAH15** and **PHA50** additionally showed a large quantity of 2-butenoic acid (~8–12 %). The **PHAc** sample indicated the presence of considerably high amount of methyl ester (~15 %), butyl citrate (~12.9 %), and tributyl ester (~17 %). The compositional analyses of the liquid fraction of the **PET** and block co-polymers have shown carcinogenic and toxic properties. Pyrolysis removed matrices in the **CRFC** composites which is an indication of potential recovery of the original fibers.

## 1. Introduction

Today, polymers known as bioplastics are emerging as environmentally friendly materials that have the potential to meet or exceed the functional performance of petroleum-based polymers (Schrader et al., 2015), and can be blended with a large number of bio- and petrochemical-based polymers to achieve desired properties and functionalities for a wide range of applications (Pei et al., 2011; Schrader et al., 2015). Hydrocarbons derived from renewable sources can be polymerized to make bio-based polyethylene (**bioPE**) and polyethylene terephthalate (**bioPET**), which are non-biodegradable, while other bioplastics like polylactic acids (**PLA**) and polyhydroxyalkanoates (**PHA**) are biobased and biodegradable (Narancic et al., 2020). For instance, the two latter compounds are produced by bacteria, similarly to several other chemicals (*e.g.*, succinic acid, 1,3-propanediol.) (Chen, 2010). **PHA** has the particularity of being polymerized directly by bacteria as a type of carbon source, which makes it interesting as its properties can be tailored through changing process parameters during bacterial growth, especially feeding (Kenny et al., 2008; Palmeiro-Sánchez et al., 2019).

Currently, **PLA** and **PHAs** are key elements for the bioplastics market, with **PLA** at the forefront of industrial production. This polymer is chemically synthesized and it is used in a range of applications, mainly within the biomedical industry. However, due to constraints such as fragility, low thermal stability, and low impact strength, **PLA** is not suitable for several intended uses (Szacherska et al., 2021). In this regard, **PHAs** can be good candidates, and in fact its production is expected to double by 2024 in comparison with 2019 (Szacherska et al., 2021), as PHAs gain attention in the biodegradable polymer market due to their high biodegradability and versatility. They display sufficient functional properties to replace some of the synthetic plastics used worldwide today, especially in the substitution of **PET**, which is widely used from soft drink bottles to casing of electronics (RameshKumar et al., 2020). One of the challenges related to the use of bioplastics is the low heat resistance and poor impact resistance, both of which can be potentially improved with plasticizers and by blending with oil-based plastics, at the cost of inhibiting subsequent recycling. Since biodegradable bioplastics are blended with synthetic plastics and binders to achieve commercially functional properties, the environmental fate and biodegradation properties of these modified bioplastics are either scarce or unknown (Boey et al., 2021; Miao et al., 2021; Pei et al., 2011; Polman et al., 2021).

Efficient waste management aims at the maximum conservation of resources and minimization of toxicity. However, the addition of multilayer plastics and bioplastics to industry increases the complexity and economic *de facto* infeasibility of the primary and mechanical recycling methods. These methods require uncontaminated feeds, or the decontamination and separation of plastic mixtures, that make these approaches less favorable (Papari et al., 2021). Unlike mechanical recycling, chemical recycling – pyrolysis, can tolerate higher levels of contamination in the feed and produce chemicals and fuels due to intrinsic properties of plastic similar to petroleum fuels (Al-Salem et al., 2017; Al Rayaan, 2021). However, in determining the appropriate methods for chemical recycling, factors such as the amount of plastic wastes, quality of end-products, cost, energy balance, and effect on the environment need to be taken into account. The high and homogeneous heating rate seen in fluidized bed reactors can be a viable option as it produces less soot and high amount of valuable polymers from different types of plastics, and can be upscaled to recycle great amounts of plastic waste (Kaminsky, 2021). Thus, pyrolysis is acknowledged as the most economically viable (Pacheco-López et al., 2021; Rudin and Choi, 2013) and environmentally friendly method of chemical production from plastic waste yielding a high-value product (Papari et al., 2021).

For plastic wastes, pyrolysis is found to be the most suitable process for conversion to clean solid, high-value liquid, and gaseous products as it is considered as a precursor to the combustion and gasification processes (Singh et al., 2020a). Several studies (Cahyono and Ika Fenti, 2017; Cocchi et al., 2020; Hakeem et al., 2018; Singh et al., 2020b; Singh et al., 2019; Williams and Williams, 1997) have explored different pyrolysis modes for pure and mixed plastics such as polypropene (**PP**), polystyrene (**PS**), polyethylene terephthalate (**PET**), mixed plastic waste (MPW), and their products at different temperatures between 450 and 550 $^{o}$C, associated with producing valuable tars (Yansaneh and Zein, 2022). The researchers measure the char yield at 5–25 %, and the pyrolysis oil to contain aromatics with a low amount of sulfur and nitrogenous compounds. Pyrolysis is defined as either slow or fast based on the heating rate (~10 and ~100 $^{o}$C/s for slow and fast pyrolysis, respectively) (Maqsood et al., 2021). The fast pyrolysis of polymers results in fewer secondary reactions and side products. Therefore, depending on the polymers and process parameters, it is possible to obtain valuable waxy products, oil, gas, or monomers in continuous mode fast heating rate reactors (Kaminsky, 2021). However, little is known about tar formation in the fast pyrolysis of biomass, waste, and plastics due to the complexity of tar sampling and analysis. Moreover, there is a lack of knowledge on primary tar quantification for well-defined pyrolysis experiments. The formation of tars depends strongly on the operational conditions of pyrolysis (Trubetskaya et al., 2019). Previous research reports that during fast pyrolysis of biomass the primary tars are predominantly aliphatic and oxygenated (ketones, aldehydes, or carbon acids), being highly reactive at temperatures above 600 ℃ (Evans and Milne, 1987; Fuentes-Cano et al., 2013; Hayashi et al., 1992). The substituted phenols (bi- and trifunctional monoaromatics) are formed from lignin in a temperature range of 200–500 ℃ (Wolfesberger-Schwabl et al., 2012). The secondary tars are composed of alkylated mono- and diaromatics including heteroaromatics like pyridine, furan, dioxin, and thiophene. The tertiary tars are formed from homolytic cleavage of the secondary tar at temperatures above 800 ℃ and include naphthalene, phenanthrene, pyrene, and benzopyrene (Evans and Milne, 1987; Fuentes-Cano et al., 2013; Hayashi et al., 1992; Wolfesberger-Schwabl et al., 2012). In kinetic models of biomass, the total tar yield is represented by two main primary tar compounds, *i.e.*, acetol and catechol, in gasification (Fuentes-Cano et al., 2016; Umeki et al., 2010) or by three compounds, *i.e.*, acetol, toluene, naphthalene in devolatilization (Umeki et al., 2010). Another kinetic model showed that the most abundant tar compounds were catechol, *o*-cresol, and salicylaldehyde in wood gasification (Fuentes-Cano et al., 2016). The kinetic model of Jess (1996) showed that benzene is the key component of the thermal decomposition of aromatic hydrocarbons, and naphthalene is a precursor of soot formation in gasification. However, no fundamental research can be found in the literature on bioplastic thermo-chemical characteristics and products including tars and solid char. Thus, it is necessary to investigate the thermochemical

characteristics of bioplastics with chemical composition and amount of products to explain the environmental effects.

This research was motivated by the societal need to combine traditional processes like pyrolysis with novel bio-based materials to reduce plastic waste, as a continuation of the previous work (Trubetskaya et al., 2022). The lack of information on the thermochemical conversion of bioplastic materials, whose industry adoption is increasing each day, emphasizes the need for research on the thermal characterization of these materials. Researching the pyrolysis of bioplastic as a precursor and promising method to thermochemical processes is a legitimate starting point to gain more insight into the environmental effects with sustainable energy, and chemical recovery and production. In this manner, pyrolysis has been chosen to investigate the pyrolysis products of various plastics. The novelty of the present research relies on the fast pyrolysis of the synthetic plastics and bioplastics, as opposed to existing studies focused on slow pyrolysis. Therefore, this study aims at filling this gap by investigating the fast pyrolysis products (biochar and tar) obtained at temperatures seen in industrial recycling facilities (500 $^{o}$C), and often preferred for bio-oil production.

## 2. Methodology

### 2.1. Bioplastic production

The mixed microbial cultures able to accumulate **PHAs** were selected in aerobic sequential batch reactors (SBRs) of 1.8 L operating in 12 h cycles at three different temperatures, in particular 15, 30, and 48 °C. The temperature was measured and acquired by a digital meter coupled to an infrared membrane probe (Hach, US). The reactors were fully aerated and stirred by the passing-through air flow using an air pump (KNF, Germany) coupled to a diffuser system (Hagen, Canada) at the bottom of the reactors. The dissolved oxygen (DO) in the reactors was measured and acquired using a digital meter with a luminescent probe (Hach, US). The pH was not controlled yet it was measured (Hach, US). The $NH_4^+$, PHAs, VFAs, total solids (TS), and volatile solids (VS) were also measured during the daily operation and also during the characterization of the enrichment cycles.

Every other operational condition in the 3 identical SBRs was maintained the same. For instance, the organic loading rate was per cycle 58.5 Cmmol $L^{-1}d^{-1}$ of acetic acid, 18 Cmmol $L^{-1}d^{-1}$ of propionic acid, and 13.5 Cmmol $L^{-1}d^{-1}$ of butyric acid, and hence a total of 90 Cmmol $L^{-1}d^{-1}$. Both the hydraulic and solids retention times were 1 day. The aerobic dynamic feeding strategy was followed such as to apply a selective pressure on the microbial community. The organic carbon fraction of the feed was composed of a mixture of volatile fatty acids (VFAs): acetate (Ac), propionate (Pr) and, butyrate (Bu) at a constant composition of 65, 20 and, 15 Cmol. %, respectively. A feeding C:N ratio of 7.3 Cmol:Nmol was applied. Allylthiourea (ATU) was also added to inhibit the nitrification activity and avoid the subsequent oxidation of the ammonia supplied to the reactor. The solely change in temperature, *i.e.*, 15 ºC *vs.* 50 ºC, led to the selection of two different types of mixed microbial cultures and, therefore, two different types of **PHAs** in terms of composition and properties, *i.e.*, **PHA15** and **PHA50**. A commercially available sample, **PHAc** (GlasPort Bio) was used for comparison.

Once the mixed microbial cultures were selected at each one of the temperatures, fed-batch tests were performed to maximize the **PHA** content in the bacterial cells. For this purpose, the nitrogen supply was limited while the carbon source was provided in excess to favor the **PHA** accumulation inside the bacterial cells.

An extensive description of the operation of the reactors can be found in a publication in press (Palmeiro-Sánchez et al., 2022). The biomass from the accumulation trials was frozen at −80 °C and freeze-dried subsequently. A known amount of freeze-dried biomass was mixed with chloroform 99.8 % (Merck, US). The mixture was kept in a shaker at 150 rpm for 3 days at a constant temperature of 37 °C. Afterwards, the separation of the solid and liquid phases was done by filtration using solvent-resistant materials. The clean liquid phase was allocated in glass containers in a safety fume-hood. The chloroform was evaporated and the **PHA** films were formed on top of the glass surface. The thin film samples were cut the small pieces (<0.5 mm) prior to pyrolysis experiments.

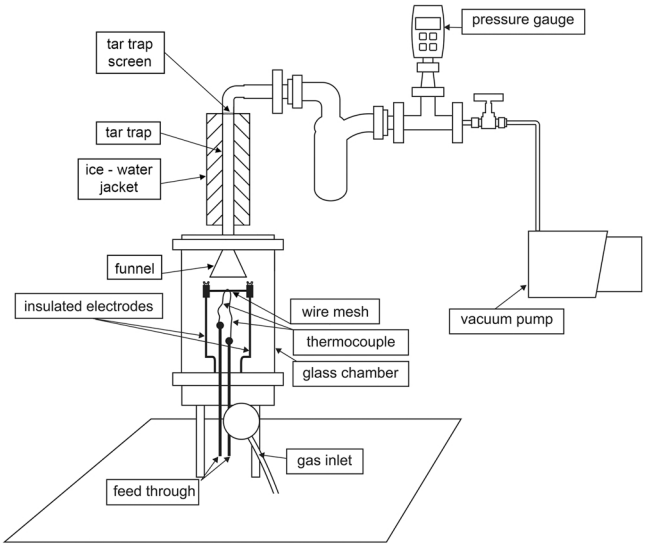


**Fig. 1.** Schematic of wire mesh reactor.

### 2.2. Synthetic plastics

Carbon fiber reinforced composites (**CFRC**) which consist of carbon fibers integrated into a plastic matrix that are mixed epoxy resins with thermoplastics were provided by SiC-Processing Ltd (Hirschau, Germany). Components made of carbon fiber reinforced composites (**CFRC**) were previously used in aviation and wind energy sector (Oliveux et al., 2015; Pakdel et al., 2021). The **CFRC** products were shredded and sieved down to two classes (< 500 μm; > 2 mm). The two block co-polymers; a 793 kg/mol **PS-b-P2VP** (440 kg/mol PS, 353 kg/mol P2VP) and a 893 kg/mol **PS-b-P4VP** (650 kg/mol PS, 243 kg/mol P4VP) were purchased from Polymer Source (Quebec, Canada) for this study. The block co-polymers were ground prior to the pyrolysis experiments. The water bottle (DASANI, US) was made from an hybride **PET** material using a mixture of plant and synthetic polymers. The central part of the **PET** water bottle was cut into small granules (<1 mm) prior to the pyrolysis experiments.

### 2.3. TGA and DSC analyses

The thermal analysis of the **PHA** and block co-polymer samples was carried out using a PerkinElmer 4000 Differential Scanning Calorimeter (Waltham, MA, USA). Approximately 5 mg of sample weighed with an analytical balance (ME54, Mettler Toledo, USA) were hermetically sealed in an aluminum pan and underwent heat-cool-heat ramps between the temperatures of −20 $^{o}$C and 200 $^{o}$C. The average melting temperature ($T_m$), cold crystallization temperature ($T_c$), and average glass transition temperature ($T_g$) were determined by applying ASTM D3418 – 15 standard. Pure nitrogen was used as a purge gas at a flow rate of 20 mL $min^{-1}$.

DSC analysis of **CRFC** and **PET** plastic samples was carried out in a temperature range of − 20–445 $^{o}$C. The average melting temperature ($T_m$), cold crystallization temperature ($T_c$), and glass transition temperature ($T_g$) were not observed in the cooling cycle and second heating cycle due to possible thermal degradation of the samples in the temperature range. Therefore, both melting temperature ($T_m$) and glass transition temperature ($T_g$) were reported from the first heating cycle.

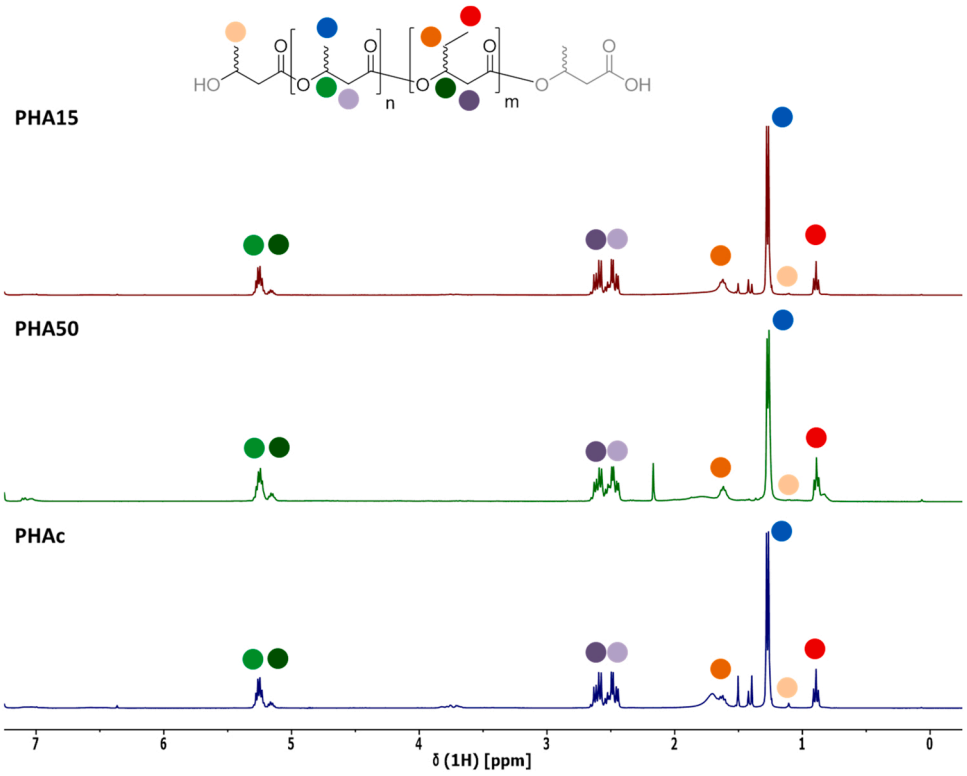


**Fig. 2.** $^{1}$H NMR spectra of PHA15, PHA50, and PHAc.

Samples of **PHA**, block co-polymer, and **CFRC** were pyrolyzed in nitrogen at a constant heating rate of 10 °C/min from room temperature to 500 °C in a PerkinElmer 4000 Thermogravimetric Analyzer (TGA). The amount of initial sample was kept low at 5 (±0.5) mg and the nitrogen flow into the TGA furnace was set to 100 mL min$^{-1}$.

### 2.4. Wire mesh reactor

A wire mesh reactor (WMR) was used to pyrolyze all samples under high heating rate (~$10^2$ °C s$^{-1}$) conditions. The WMR used herein comprised a wire mesh, conductive electrodes, a welding machine as a power source, a thermocouple, a glass chamber to control the pyrolysis ambient, a funnel to channel pyrolysis products, a tar trap, a pressure gauge, and a vacuum pump, as represented in Fig. 1. The existing WMR is comprehensively detailed elsewhere (Akın et al., 2020; Gürel et al., 2022; Magalhães et al., 2021), and has been modified herein to allow continuous tar collection. A sweep inert gas ($N_2$) was supplied from the bottom of the chamber at a constant flow rate to flush the pyrolysis products from the hot wire mesh zone; thus, the secondary cracking, possible polymerization of tar products, and secondary reactions of volatiles with the char left on the mesh were greatly reduced. The hot pyrolysis products were passed through a funnel on top of the mesh, a tar trap cooled by ice-water, and a tar trap screen to capture condensable tar products.

In the present study, the two layers of wire mesh and the tar trap screen were washed with acetone to remove any deposits of contamination prior to each experiment. The sample, approximately 15 mg, was evenly distributed as a thin layer in between the two wire meshes to minimize the non-uniform heat distribution within the sample. The pyrolysis of samples was conducted at atmospheric pressure and the sweep gas ($N_2$) flow rate was set to 4 L min$^{-1}$ to flush the pyrolysis products to the funnel. The sample was heated to the temperature of 500 °C at a heating rate of ~$10^2$ °C s$^{-1}$ and held at the peak temperature for 45 s to ensure that pyrolysis was completed. The wire mesh along with the solid residue was gently removed from the electrodes after the experiment and reweighed, to obtain the char yield. The funnel, tar trap, and tar trap screen were detached from the WMR, to retrieve the tar for further analysis.

The char yield measurements were performed at least in triplicate to obtain single point data. The experimental char yield, $Y_{exp}$, was calculated using Eq. 1.

$$Y_{exp}(wt.\%) = \frac{m_{f(mesh+char)} - m_{i(mesh)}}{m_{i(sample)}} \times 100 \quad (1)$$

where $m_{f(mesh+char)}$ is the final total mass of the mesh and char, $m_{i(mesh)}$ is the initial mass of the mesh, and $m_{i(sample)}$ is the mass of raw sample placed in between the meshes.

### 2.5. GC–MS characterization of collected tars

The condensable tar products in the funnel, tar trap, and tar trap screen were collected by washing out these components with acetone, and the solubilised collected tar products were analyzed by gas chromatography coupled to mass spectrometry (GC–MS). The funnel, tar trap, and tar trap screen were washed with 20, 15, and 5 mL of acetone (ISOLAB®, purity >99.8 %), respectively. The solutions were concentrated using a rotary evaporator at 40 °C and 40 rpm under vacuum. The analysis of tar compounds was performed on a single quadrupole gas chromatography-mass spectrometry (GCMS-QP2020, Shimadzu Corporation, Japan) equipped with a DB-5MS capillary column (0.25 mm internal diameter, 0.25 μm film thickness, Agilent Technologies, USA). In each analysis, 0.5 μL of the sample was injected into the instrument at a 1:1 split ratio. Helium was used as a carrier gas with a constant flow of 1 mL min$^{-1}$. The temperature of the injector and interface was kept at 250 °C and 300 °C, respectively. The following temperature profile was run: (i) 50 °C for 2 min, (ii) ramp up at 1.5 °C min$^{-1}$ to 160 °C, (iii) ramp up at 6 °C min$^{-1}$ to 230 °C, (iv) ramp up at 8 °C min$^{-1}$ to 280 °C, and (v) 280 °C for 5 min. The mass spectrometer scanned the range from $m/z$ 35 to $m/z$ 250 in a scan rate of 0.6 scans s$^{-1}$. Chromatographic peaks were identified utilizing the NIST27, NIST147, and WILEY W9N11 mass

spectral data libraries.

### 2.6. Statistical modeling

Statistical modeling was performed using SAS JMP 15.0 (Frankfurt, Germany). Analysis of variance (ANOVA) was performed to evaluate the effect of the feedstocks on the results of component analysis from GC–MS analysis. Multiple linear regression using variability chart representation was performed to evaluate the relationship between feedstocks and tar composition. All analyses were performed at significance level with $\alpha = 0.05$.

### 2.7. NMR analysis

Samples of around 15 mg were dissolved in 600 µL $CDCl_3$; $^1H$ NMR spectra were recorded at 27 ℃ on a Bruker 400 MHz instrument equipped with TopSpin 2.1 software applying the Bruker zgpulse program in DQD acquisition mode, with NS = 64; D1 = 8 s. Nuclear magnetic resonance (NMR) data were processed with MestreNova; spectra were referenced to the residual signals of $CDCl_3$ (7.26 ppm).

### 2.8. Size exclusion chromatography analysis

The molecular weight values of **PS-b-P2VP** and **PS-b-P4VP** were adopted from previous investigations where NMP was used as a solvent during SEC analysis (Varshney et al., 1993). The molecular weight of **PET** bottle polymer was determined using chloroform as a solvent, as previously discussed (Demirel and Daver, 2009).

Number average molecular weight ($M_n$) and weight average molecular weight ($M_W$) of **PHAs** were determined by size exclusion chromatography (SEC) (Knauer Smartline, Germany) using a refractive index detector. The samples were dissolved in $CHCl_3$ within a concentration range between 0.2 and 0.3 (m/V) %. A Phenomenex Phenogel Linear LC Column (300 × 7.8 mm, Phenomenex, US) was used, with $CHCl_3$ as eluent at a flow rate of 0.5 mL $min^{-1}$ at 30 ℃. Each injection was of 100 µL and duplicates were performed for each sample. The calibration was done with 12 samples of polystyrene standards (Supelco, US) within the range of 0.37–2520 kDa.

### 2.9. SEM analysis

The morphology of the non-treated wire mesh and char samples from fast pyrolysis was characterized using Scanning Electron Microscopy (SEM). Samples were placed on carbon tape and coated with Au/Pd before analysis. Imaging was performed using a 400F instrument (FEI Quanta, USA) under high vacuum.

## 3. Results and discussion

### 3.1. NMR and GPC analysis

**PHA15, PHA50,** and commercial **PHAc** are characterized as poly(3-hydroxybutyrate-co-3-hydroxyvalerate), with the valerate motif accounting for approx. 16 ± 1 % in the three samples. Sample purity is of around 90 % in NMR analyses for all three samples. Fig. 2 shows the $^1H$ NMR spectra of the two samples with a representative structure of the poly(3-hydroxybutyrate) in the study. Gel permeation chromatography (GPC) analyses of the three bioplastics suggest that they are all of the same molecular weight regime, *i.e.*, exhibit molecular sizes of around 170–270 kDa, as such corresponding to the results of the NMR analyses. The higher polydispersity found for **PHA50** corresponds to the fact that the $^1H$ NMR of this sample shows a rougher baseline, hinting as such overall at a less controlled polymerization condition. This could occur due to production of more heterogenous composition of **PHA** at 50 °C by the mixed organism set compared to the polymerization by the microorganisms at 15 °C as observed in a previous article (Palmeiro-Sánchez et al., 2022) (Fig. 3).

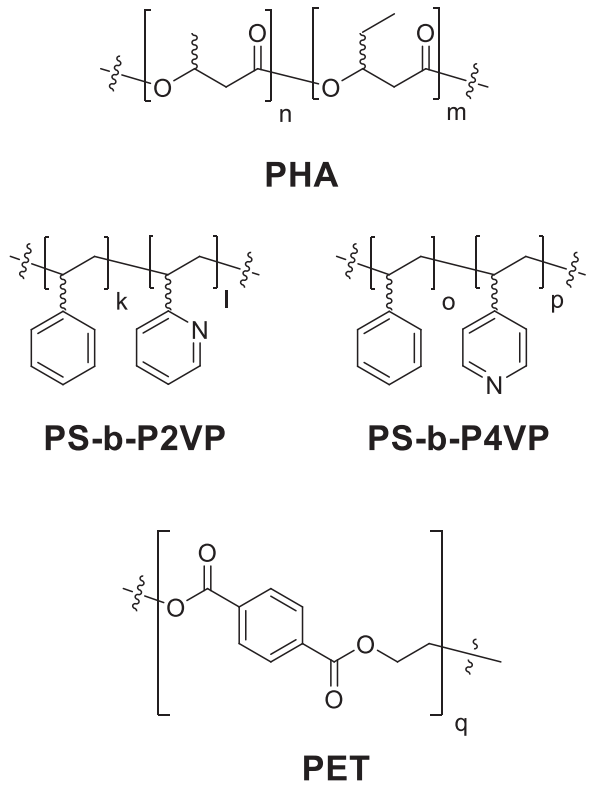


**Fig. 3.** Structural representations of polymer types used in this study; detailed structural information regarding the epoxy resin used within the **CFRC** was not disclosed.

**Table 1**
Size exclusion chromatography (SEC) analyses of PHA15, PHA50, PHAc PS-b-P2VP, PS-b-P4VP, and PET bottle polymer.

| Sample | $M_n$ $10^3$ g $mol^{-1}$ | $M_w$ $10^3$ g $mol^{-1}$ | PDI |
|---|---|---|---|
| **PHA15** | 169 | 320 | 1.9 |
| **PHA50** | 272 | 655 | 2.4 |
| **PHAc** | n.d. | 440 – 600 | n.d. |
| **PS-b-P2VP** | 440 (PS)<br>353 (VP) | 943 | 1.2 |
| **PS-b-P4VP** | 650 (PS)<br>243 (VP) | 1056 | 1.2 |
| **PET** bottle plastic | 26 | 52 | 2.0 |

**Table 2**
Average thermal transition results obtained *via* DSC.

| Sample | $T_g$ Second Heat (°C) | $T_c$ (°C) | $T_m$ First Heat (°C) | $T_m$ Second Heat (°C) |
|---|---|---|---|---|
| **PHA15** | 43 | 12 | 142 | – |
| **PHAc** | – | 98 | 130 | 131 |
| **PS-b-P2VP** | 86 – 94 | 90 | – | – |
| **PS-b-P4VP** | 106 – 155 | 103 | – | – |
| **CRFC** 500 µm | 140 | – | 315 | – |
| **CRFC** 2000 µm | 152 | – | 302 | – |
| **PET** bottle plastic | 75 | – | 243 | – |

### 3.2. TGA and DSC characterization

The thermal decomposition temperatures of the **PHA**, block copolymer, and **CFRC** samples were studied using thermogravimetric analyzer (TGA), and the results are shown in Figs. S.7 – S.9 of the Supporting information. The thermal events of glass, crystallization, and

melting transitions of **PHA**, block co-polymer, **CFRC**, and **PET** bottle samples obtained *via* differential scanning calorimetry (DSC) are summarized in (Table. 1).

Table 2, and the scans are shown in Figs. S.1–S.6 of the Supporting Information. Thermogravimetric analysis (TGA) indicated that the weight losses of **PHA15**, **PHA50**, and **PHAc** showed decomposition in a single-step starting from 141, 186, and 198 °C, respectively (see Fig. S.7). The thermal decomposition of **PHA15** started earlier and reached the maximum decomposition rate at 222 °C. On the other hand, the peak temperatures of **PHA50** and **PHAc** samples were observed at 251 and, 244 °C, respectively. The DSC analysis of the **PHA15** sample indicated that the $T_g$ and $T_c$ were observed at 43, and 12 °C, respectively (see Figs. S.2 and S.4). The melting temperature was not observed in the second heating, while it exhibited a broader melting range starting between 142 °C and 158 °C in the first heating (see Figs. S.1 and S.3). The **PHAc** sample exhibited a $T_c$ at 98 °C, and $T_m$ range starting at 130 °C in the first heating, and 131 °C in the second heating (see Figs. S.1–S.3); however, it showed no glass transition behavior in the second heating. For amorphous plastics, the $T_g$ is the most important thermal parameter defining the range of applications that are often used in food packaging because the lack of crystallites in the polymer structure generally permits superior optical transparency. The low glass transition temperature and high melting temperature could indicate the presence of higher medium-long chains compared to short chains, and the importance of the ratio of high melting temperature poly(3-hydroxybutyrate) (PHB) to low melting temperature 3-hydroxyvalerate (3HV) units (Obruca et al., 2014; Raza et al., 2018).

The derivative weight curves of TGA showed a slight shoulder at lower temperatures for block co-polymer samples which is related to the separation of the **P2VP** and **P4VP** homo-polymers from the **PS** block as seen in Figure S.8. The first stage degradation of **PS-b-P2VP** and **PS-b-P4VP** block co-polymer samples took place when the temperature reached 152 °C and 136 °C, respectively. The main breakdown of **PS-b-P2VP** and **PS-b-P4VP** started at 344 °C and 334 °C, with peak temperatures observed at 421 °C and 417 °C, respectively. The block co-polymers presented two glass transition temperatures, indicating that the block co-polymers were microphase separated. The two glass transition temperatures of **PS-b-P4VP** block co-polymers were obtained at 94 °C, and 155 °C, respectively, as seen in Figure S.4. The higher glass transition temperature was attributed to the P4VP block, and the lower to the PS block, as previously reported (Chu et al., 2013). In our case **PS-b-P2VP** block co-polymers showed two similar $T_g$ values at around 90 °C (see Fig. S.2), thus it was difficult to discriminate the miscibility between PS and P2VP segments, in line with previously reported results (Hsu et al., 2021). A slight crystallization peak during cooling was observed at 90 °C and 103 °C for **PS-b-P2VP** and **PS-b-P4VP**, respectively (see Fig. S.2). The **PS-b-P4VP** and **PS-b-P2VP** showed no melting behavior in the temperature range of −20 to 200 °C (see Figures S.1 and S.3). Thus, DSC and TGA results of block co-polymers (**PS-b-P4VP**, and **PS-b-P2VP**) used herein suggest greater thermal melting stability than bioplastic samples.

The TG and DTG curves of the **CRFC** with particle size below 500 μm showed that the thermal decomposition started at around 260 °C, and reached the highest conversion rate at around 381 °C (see Figure S.9). The char yield of the **CFRC** sample obtained in TGA was around 80 %, which was higher than that of the char obtained in the WMR. The lower char yield in WMR was attributed to strong deformation of the sample at high heating rates (Trubetskaya et al., 2015). The **CRFC** with particle size below 500 μm showed a $T_g$ (140 °C) and a $T_m$ (315 °C) which were higher than those observed for the other polymeric samples. The **CRFC** sample of particle size larger than 2000 μm showed $T_g$ (152 °C) and $T_m$ (302 °C) which emphasized the importance of particle size on the thermal properties of **CRFC** composites (see Figure S.6). Furthermore, the thermal decomposition range (375–390 °C) obtained from DSC curves of **CRFC** samples matched with the peak of DTG curve (381 °C, proving the thermal decomposition process (see Figures S.5, S.6, and S.9). Previous works have suggested that a polymer matrix of the investigated **CRFC** could contain poly (ether ether ketone) (**PEEK**) with carbon fibers, with a $T_g$ of approximately 140 °C and a $T_m$ of 320–360 °C (Doumeng et al., 2021; Lu et al., 2019). Chukov et al. (2019) have reported the appearance of the glass transition temperature in the polyphenylene sulfide (**PPS**) matrix with the addition of carbon fibers into the composite. Serenko et al. (2017) emphasized the importance of carbon fiber diameter and formation of dispersed phase of polymers in the composite leading to strong changes in $T_g$. They have also hypothesized that the $T_g$ can decrease or disappear with the increasing content of carbon fibers and nanoparticles. This corresponds to previous results in which the particle size of the **CRFC** composite was decreased during hammer milling, the mechanical properties of carbon fibers increased (Li and Englund, 2017). The addition of nanofillers into the **CRFC** matrix of large particles is known to constrain the segmental motion of polymeric fraction and reduce the free volume so as to increase the $T_g$ (Gojny and Schulte, 2004). Thus, the optimization of the $T_g$ and $T_m$ in **CRFC** samples strongly depends on the dispersion degree, homogeneity, and spacing between carbon fibers (Tang et al., 2013).

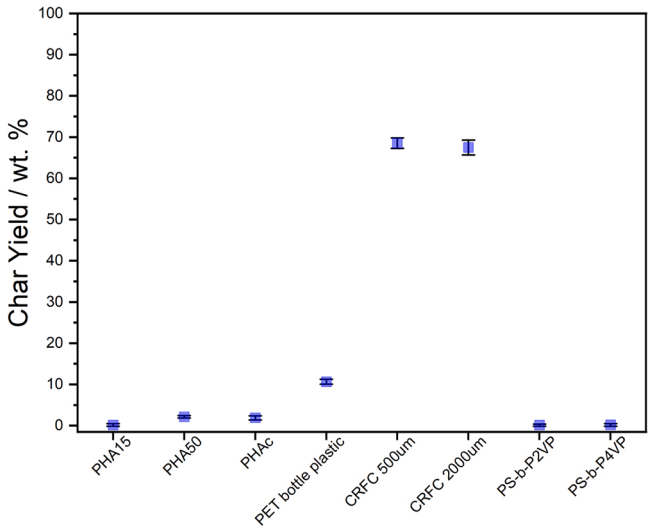


**Fig. 4.** Char yields (wt. %) of PHA15, PHA50, PHAc, PET bottle plastic, CRFC 500 μm, CRFC 2000 μm, PS-b-P2VP, PS-b-P4VP from fast pyrolysis in the wire mesh reactor.

With respect to **PET** of the plastic bottle, the glass transition (75 °C), and melting (243 °C) temperatures were higher than it was observed for both tested **PHA** samples. The results were in line with the findings of previous researchers (Cheng et al., 2016), and the minimum temperature for thermal decomposition (>380 °C) observed in DSC curve (see Fig S.5) was similar to the TG-DSC results of J. Li et al. (2021) and Y.F. Li et al. (2021). The low $T_g$ of **PHA** is known to limit its market expansion to replace higher $T_g$ materials such as **PET** (Nguyen et al., 2018).

### 3.3. Char yield from WMR pyrolysis

The char yields of the synthetic plastic (**PET**), bioplastics (**PHAs**), block co-polymers, and **CFRC** samples are represented in Fig. 4.

The char yields of the **PHA** bioplastics and the block co-polymer samples were by far the lowest among all samples. Moreover, it should be noted that the char yields of bioplastic samples were slightly above those of block co-polymers. The char yields from bioplastic **PHA15** and **PHAc** samples were 2.13 ± 0.29 and 1.89 ± 0.50 wt. %, respectively. This indicates the high conversion of **PHA** samples into the volatile fraction. The similar char yields of **PHA** samples were attributed to similar amounts of hydroxyvalerate content, and impurities. The yields from **PHA** sample pyrolysis were notably lower than those from synthetic plastic. Similarly, the complete degradation of similar

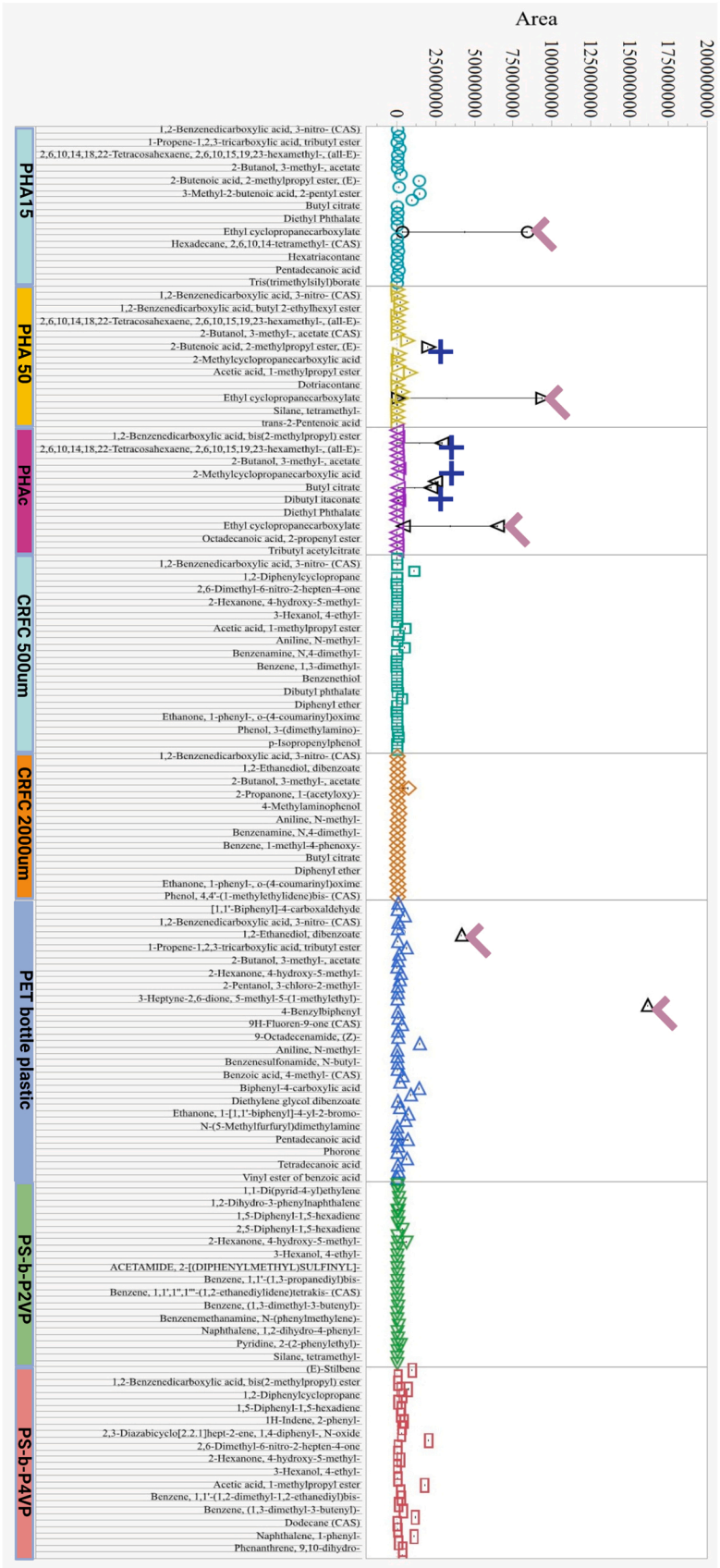


**Fig. 5.** Main tar compounds detected in tar samples from PHA15, PHA50, PHAc, PS-b-P2VP, PS-b-P4VP, PET bottle plastic, and CRFC according to the variability analysis using JMP software.

bioplastic polymers, leaving behind the metallic impurities, was reported previously by several researchers (Ariffin et al., 2010; Kim et al., 2006; Modi et al., 2011).

The char yields obtained from block co-polymers **PS-b-P2VP** and **PS-b-P4VP** were 0.11 ± 0.27, and 0.19 ± 0.32 wt. %, respectively. This was due to the optimally selected operating temperature at 500 ℃ of the WMR that led to the conversion of both block co-polymers to the liquid fraction (above 96 wt. %) and a small fraction of gas and solid char (Maafa, 2021). Previous research reported the formation of styrene and vinylpyridine-containing liquid compounds when the operating temperature of the fixed bed pyrolysis reactor was selected below 581 ℃ (Demirbas, 2004).

The char yield of **PET** (10.7 ± 0.60 wt. %) obtained from the water bottle was higher than those of the **PHA** bioplastics and block co-polymers, while lower than those of **CFRC** samples. Saha and Ghoshal (2006), and Singh et al. (2020a,b) conducted pyrolysis of polyethylene terephthalate at 450–600 °C in a thermogravimetric analyzer and observed char yields of 10–13 wt. %, and 15–18 wt. %, respectively. Similarly, Eriksen et al. (2019) reported the char yield of PET samples at 12–15 % at 700 °C and correlated the yield with the ash formation due to incomplete degradation of aromatics in **PET**. The results herein for synthetic plastic char yields were similar to those observed by the authors.

The char yields of **CFRC** with particle size <500 μm and > 2000 μm were obtained as 68.5 ± 1.28 wt. % and, 67.5 ± 1.79 wt. %, respectively. In the literature, the high heating rate and low residence time were correlated with the incomplete process which resulted in higher char yields (Ogunkanmi et al., 2018). However, the char yields in this study have shown that pyrolysis was completed for both particle sizes of **CFRC** samples. In fact, the weight loss in the **CRFC** samples was attributed to the devolatilization of epoxy resin in the composite matrix, rather than the decomposition of carbon fibers (Meyer et al., 2009) during the described pyrolysis conditions.

### 3.4. Tar yield and composition

The results of the GC–MS analyses were analyzed using JMP software and are shown using the variability chart in Fig. 5. Only compounds with a spectral match quality greater than 85 % and an abundance greater than 0.5 % were considered in the statistical data analysis. The compounds with the largest compound area are marked to highlight the significant differences in the tar composition among various polymeric samples.

The tar from pyrolysis of **PS-b-P2VP** contained larger quantities of 4-hydroxy-5-methyl-2-hexanone (3.1 %), 2,5-diphenyl-1,5-hexadiene (1.8 %), 2-(2-phenylethyl)-pyridine (1.2 %), and bibenzyl (0.6 %). The liquid fraction of **PS-b-P4VP** showed a more heterogeneous structure with dominating compounds such as 1-methylpropyl ester acetic acid (5.8 %), 2,5-diphenyl-1,5-hexadiene (6.5 %), 1-phenyl-naphthalene (4.7 %), dibenzyl (3.8 %), 1,2-dihydro-3-phenylnaphthalene (2.4 %), 1,4-diphenyl-2,3-diazabicyclo [2.2.1] hept-2-ene (1.1 %), and 1,5-diphenyl-1,5-hexadiene (0.9 %). The tar fractions from pyrolysis of **CRFC** showed a high quantity of phthalic acid (~ 15 %) and *sec*-butyl acetate (~ 11 %) that is known to be used as a thinner and a hardener of polyamine matrix (Sokoli et al., 2017; Streitwieser and Heathcock, 1981). The polymer matrix of polyimide is known to include such compounds as 4-hydroxy-5-methyl-2-hexanone (31 %), and aniline (1.5–2.8 %) which were also determined in the tar composition from pyrolysis of both **CRFC** samples (Belaabed et al., 2010). Previous investigations indicated the need to develop safety procedure measures for the examination of the composition of gas phase and liquid products during pyrolysis of polymer-based carbon fibers composites (Lefeuvre et al., 2017; Seiler and Teipel, 2018). Despite the fact that in the present study, the liquid fraction from pyrolysis of **CRFC** did not contain toxic compounds, the composition of the polymeric matrix in the **CRFC** composites varies from one application field to another (Lefeuvre et al., 2019; Sauer and Carbon Composites e.V, 2019; Stockschläder et al., 2018). Thus, it is recommended to provide the compositional analysis of the **CRFC** composites prior to any further recovery treatment of carbon fibers.

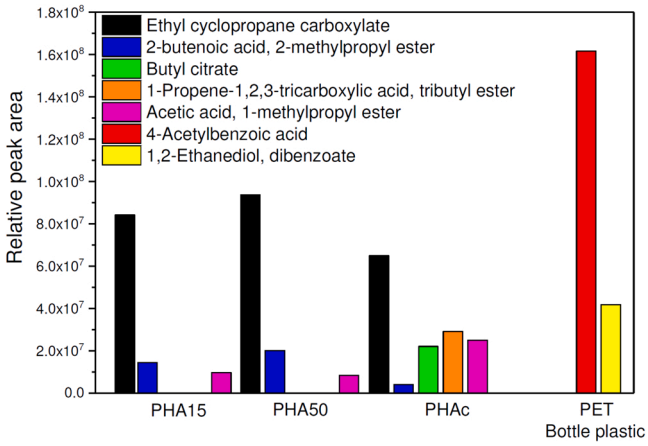


**Fig. 6.** Statistical model for the tar composition using GC–MS data of PHA15, PHA50, PHAc, and PET bottle plastic samples. Relative peak area of main tar compounds obtained from statistical model.

The tar composition of **PHA** samples and **PET** bottle showed significant compositional differences with respect to the largest relative area of peaks compared to all reacted samples. The main compounds in the tar samples of **PHA15**, **PHA50**, **PHAc,** and the **PET** plastic bottle polymer are shown in Fig. 6.

All **PHA** compounds contained a large fraction of ethyl cyclopropane carboxylate (~ 38–58 %), whereas **PAH15** and **PHA50** additionally showed a large quantity of 2-butenoic acid (~8–12 %). The **PHAc** sample indicated the presence of considerably high amount of methyl ester (~15 %), butyl citrate (~12.9 %), and tributyl ester (~17 %) than **PHA15** and **PHA50** samples. The butyl bitrate and tributyl ester were determined in the composition of liquid products from **PHA** pyrolysis and their significant presence was related to the addition of plasticizers to the **PHA** samples (Naser et al., 2021). Interestingly, similar plasticizers were detected in the structure of plastic baby bibs (Kato and Conte-Junior, 2021). This shows that **PHA** can be further tailored with respect to the desired thermo-mechanical properties using additives. The **PET** bottle polymer-derived tar contained a large fraction of 4-acetylbenzoic acid (38.9 %) that has been previously determined in a liquid product from pyrolysis at 500 ℃ (Çepelioğulları and Pütün, 2013). In addition, the **PET** bottle matrix contained a significant amount of dibenzoate 1,2-ethanediol (10.8 %) with small traces of butyl citrate which are known for their excellent properties of a plasticizer (Damayanti and Wu, 2021). Traces of compounds such as biphenyl (1.4 %) and other monomers containing biphenyl groups (~4.5 %), benzophenone (0.5 %), and *m*-terphenyl (1.3 %) were also detected.

### 3.5. SEM

The morphology of the non-treated wire mesh, raw **CRFC** samples, and selected chars obtained at 500 ℃ pyrolysis was investigated using SEM. Selected images are represented in Fig. 7. The chars of the **PET** bottle (Fig. 7b) and **CFRC** (Fig. 7e-h) could be gently collected from the wire mesh; however, **PHA** chars (Fig. 7c-d) could not be collected and were imaged on the mesh. Therefore, the untreated mesh was imaged for comparison and reference.

The surface of **PET** bottle char showed the most molten structure compared to any of the other chars, as shown in Fig. 7b. The softening of the solid char matrix and formation of a small number of pores in the WMR that is similar to the morphology of the char obtained in a fluidized bed reactor at 475 ℃ (Ahangar et al., 2021), was observed herein.

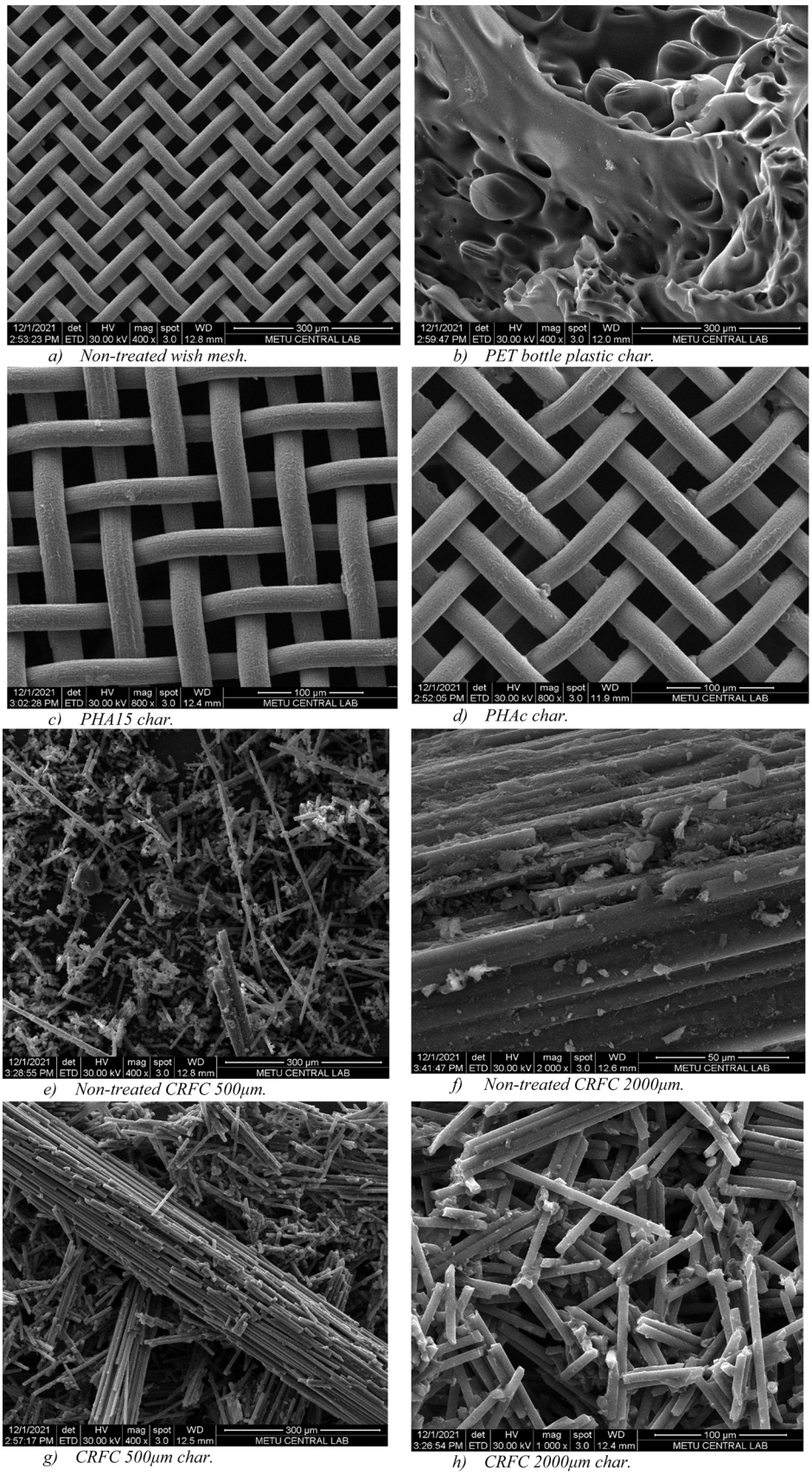


**Fig. 7.** SEM images of a) non-treated mesh, b) PET bottle plastic char, c) PHA15 char, d) PHAc char, e) non-treated CRFC 500 μm, f) non-treated CRFC 2000 μm, g) CRFC 500 μm char, and h) CRFC 2000 μm char.

This shows that the **PET** bottle plastic released gaseous and liquid products. However, the remaining solid char is a product that requires further treatment to increase the yields of value-added compounds. In comparison, neither **PHA** sample formed a solid char on the wire mesh, as shown in Figs. 7c and 7d. This indicated that through pyrolysis, **PHA** was converted completely to gaseous and liquid products. The wire mesh remained empty with minimum attachments of bioplastic solid char, which in light of the ash analysis is likely to be a reminiscent of impurities. The absence of inorganic matter and cellular structure in **PHA** samples led to a significant bridge-breaking before it started to cross-link and became fluid, similar to the fast pyrolysis of cellulose (Trubetskaya et al., 2015).

Figs. 7e and 7f show that the carbon fibers had a homogeneous structure with an equal distance between samples. However, the composition of **CRFC** samples varies and often there will be large empty spaces between carbon fibers which have a strong impact on the knife-milling process and recovery of the polymer matrix during further chemical and thermal treatment. The fast pyrolysis of small and large sized fractions showed that the polymeric matrix can be removed at 500 ℃, a fact that emphasizes the importance of the heating rate on the recovery of carbon fibers. The irregular particles from the polymer matrix were present in a small quantity and their structure was plasticised. The structure of the recovered carbon fibers did not show many differences from that of non-treated fibers. The shredding of the **CRFC** samples to 500 μm and 2000 μm sizes led to the reduction of the length of the carbon fibers that varies between 6 and 15 mm (Y.F. Li et al., 2021). However, it seems that all carbon fibers are well separated from the polymer matrix and neighboring fibers which is encouraging for pyrolysis as a post-treatment process for recovery and reuse of carbon fibers in the manufacturing of new construction materials. Another aspect for further investigation is related to the pyrolysis treatment of fibers without knife-milling that possibly will also provide equally efficient properties such as mechanical strength and fast up-reaction of the polymer matrix.

## 4. Conclusion

In the present work, the fast pyrolysis of **PET**, **PHA15**, **PHA50**, **PHAc**, **CRFC**, **VS-b-P2VP**, and **VS-b-P4VP** was carried out using a high heating rate wire mesh reactor (WMR) at 500 $^{o}$C. The physical and chemical properties of samples were analysed by NMR, SEC, and DSC analyses. The char yields were recorded, and the chars were imaged with SEM. The tar products were analysed by GC–MS for the investigation of both chemical recycling potential, and environmental effect.

- The fast pyrolysis showed a great potential to convert **PHA** thin layers into compounds that can eventually serve as building blocks for the chemical industry, *e.g.*, ethyl cyclopropane carboxylate, 2-butenoic acid, methyl ester, butyl citrate, and tributyl ester.
- The original structure of **PHA** samples contained high amounts of poly(3-hydroxybutyrate), with traces of other compounds including plasticizers in the **PHAc** sample. All **PHA** samples showed high purity with no presence of inorganic matter that led to the formation of char with yield below 2 wt. %.
- The DSC and SEC analysis have shown that **PHA** has high molecular weight with low glass transition temperature (< 55 ℃) and melting temperature (<140 ℃), compared to the **PET** bottle plastic (glass transition temperature ~ 80 ℃; melting temperature ~ 250 ℃).
- The pyrolysis of **CRFC** composites comprising synthetic polymer matrices showed promising results with respect to the recovery of carbon fibers. The fast pyrolysis at 500 ℃ led to the conversion of the polymer matrix to liquid and gaseous products, whereas the recovered carbon fibers retained their length of approximately 500 and 2000 μm, and were retained in a bundle with other carbon fibers.
- The compounds determined in the liquid fraction of both **CRFC** samples were mostly related to the presence of plasticizers and did not contain toxic or carcinogenic elements.
- The present results on the char yield after pyrolysis and char morphology showed that the shredding had a negligible impact on the properties of carbon fibers.
- The composition of the liquid fraction from pyrolysis of the **PET** bottle plastic, *i.e.,* biphenyl, benzophenone, and *m*-terphenyl, and of block co-polymers, *i.e.,* hexadiene, stilbene, and 2,5-diphenyl-1,5-hexadiene, are toxic and carcinogenic which complicates the application of such synthetic polymers within the circular economy in Europe.

The integration of new polymers, such as PHA and PLA into existing polymer waste recycling technologies, and their development is crucial to save the planet and create a sustainable economy. Thus, the formation of environmental pollutants such as soot, solid residue, and toxic pollutants like dioxins, furans, polychlorinated biphenyls, and polycyclic aromatic carbons (PAHs) should be investigated further under conditions representative of those found in chemical recycling technologies.

## Environmental implication

The current global growth of plastics production and related pollution can be slowed down by actions focused on the integration of cost and energy efficient processes for plastic reutilization and recycling. This study integrates a concept for the replacement of fossil-based plastic with bioplastic made from polyhydroxyalkanoates. Tones of composite waste containing valuable carbon fibers (**CRFC**) which accumulate on landfill of agricultural fields could be minimized using fast pyrolysis under the proposed operating conditions. Moreover, this study looked into potential replacement of environmental toxic binders in **CFRC** with the cost-efficient by-products from fast pyrolysis of bioplastics.

## CRediT authorship contribution statement

Conceptualization, A.T., T.S., F.K.; methodology, T.S., F.K., A.T.; software, S.M., A.P.; validation, A.G., D.M. and H.L.; formal analysis, A.G., A.T., F.K.; investigation, A.G., F.K., H.L., T.S., D.M., A.P. and A.T.; resources, F.K., A.T., and H.L.; data curation, A.G., D.M., A.P., and S.M.; writing—original draft preparation, A.G., A.T., T.S., and H.L.; writing—review and editing, F.K., S.M., D.M.; visualization, A.G., A.T., and S.M.; supervision, F.K. and A.T.; project administration, F.K., T.S., A.G.; funding acquisition, F.K., H.L., T.S. All authors have read and agreed to the published version of the manuscript.

## Declaration of Competing Interest

The authors declare the following financial interests/personal relationships which may be considered as potential competing interests: Anna Trubetskaya reports financial support was provided by YERUN Young European Research Universities. Feyza Kazanc reports equipment, drugs, or supplies was provided by Composite Material Characterization Laboratory, METU.

## Data availability

No data was used for the research described in the article.

## Acknowledgement

The authors acknowledge YERUN Young European Research Universities mobility award grant 2021 for the finanical support. The authors appreciate the Central Laboratory and the Composite Material Characterization Laboratory (RÜZGEM) of Middle East Technical University for their support.

## Appendix A. Supporting information

Supplementary data associated with this article can be found in the online version at doi:10.1016/j.jhazmat.2022.129696.

## References


Ahangar, F.A., Rashid, U., Ahmad, J., Tsubota, T., Alsalme, A., 2021. Conversion of waste polyethylene terephthalate (Pet) polymer into activated carbon and its feasibility to produce green fuel. Polym. (Basel) 13, 3952. https://doi.org/10.3390/polym13223952.

Akın, S.Ş., Magalhães, D., Kazanç, F., 2020. A study on the effects of various combustion parameters on the mineral composition of Tunçbilek fly ash. Fuel 275, 117881. https://doi.org/10.1016/j.fuel.2020.117881.

Al Rayaan, M.B., 2021. Recent advancements of thermochemical conversion of plastic waste to biofuel - a review. Clean. Eng. Technol. 2, 100062 https://doi.org/10.1016/j.clet.2021.100062.

Al-Salem, S.M., Antelava, A., Constantinou, A., Manos, G., Dutta, A., 2017. A review on thermal and catalytic pyrolysis of plastic solid waste (PSW). J. Environ. Manag. 197, 177–198. https://doi.org/10.1016/j.jenvman.2017.03.084.

Ariffin, H., Nishida, H., Hassan, M.A., Shirai, Y., 2010. Chemical recycling of polyhydroxyalkanoates as a method towards sustainable development. Biotechnol. J. 5, 484–492. https://doi.org/10.1002/BIOT.200900293.

Belaabed, B., Lamouri, S., Naar, N., Bourson, P., Hamady, S.O.S., 2010. Polyaniline-doped benzene sulfonic acid/epoxy resin composites: structural, morphological, thermal and dielectric behaviors. Polym. J. 42, 546–554. https://doi.org/10.1038/pj.2010.41.

Boey, J.Y., Mohamad, L., Khok, Y., Sen, Tay, G.S., Baidurah, S., 2021. A review of the applications and biodegradation of polyhydroxyalkanoates and poly(Lactic acid) and its composites. Polymers (Basel) 13, 1544. https://doi.org/10.3390/polym13101544.

Cahyono, M.S., Ika Fenti, U., 2017. Influence of heating rate and temperature on the yield and properties of pyrolysis oil obtained from waste plastic bag. Conserv. J. Energy Environ. Stud. 1, 1–8. https://doi.org/10.30588/cjees.v1i1.248.

Çepelioğulları, Ö., Pütün, A.E., 2013. Utilization of two different types of plastic wastes from daily and industrial life. J. Selcuk. Univ. Nat. Appl. Sci. 694–706.

Chen, G.-Q., 2010. Introduction of Bacterial Plastics PHA, PLA, PBS, PE, PTT, and PPP, in: Microbiology Monographs. Springer, Berlin, Heidelberg, pp. 1–16. https://doi.org/10.1007/978–3-642–03287-5_1.

Cheng, W.-D., Gu, X.-H., Song, X., Zeng, P., Wu, Z.-J., Xing, X.-Q., Mo, G., Wu, Z.-H., 2016. In-situ SAXS study on PET/ PMMT composites during tensile tests. Chin. Phys. B 25, 017802. https://doi.org/10.1088/1674-1056/25/1/017802.

Chu, W.C., Li, J.G., Wang, C.F., Jeong, K.U., Kuo, S.W., 2013. Self-assembled nanostructure of polybenzoxazine resins from reaction-induced microphase separation with poly(styrene-b-4-vinylpyridine) copolymer. J. Polym. Res. 20, 272. https://doi.org/10.1007/s10965-013-0272-8.

Chukov, D., Nematulloev, S., Zadorozhnyy, M., Tcherdyntsev, V., Stepashkin, A., Zherebtsov, D., 2019. Structure, mechanical and thermal properties of polyphenylene sulfide and polysulfone impregnated carbon fiber composites. Polymers (Basel) 11, 684. https://doi.org/10.3390/polym11040684.

Cocchi, M., De Angelis, D., Mazzeo, L., Nardozi, P., Piemonte, V., Tuffi, R., Ciprioti, S.V., 2020. Catalytic pyrolysis of a residual plastic waste using zeolites produced by coal fly ash. Catalysts 10, 1–17. https://doi.org/10.3390/catal10101113.

Damayanti, Wu, H.S., 2021. Strategic possibility routes of recycled pet. Polymers (Basel) 13, 1475. https://doi.org/10.3390/polym13091475.

Demirbas, A., 2004. Pyrolysis of municipal plastic wastes for recovery of gasoline-range hydrocarbons. J. Anal. Appl. Pyrolysis 72, 97–102. https://doi.org/10.1016/J.JAAP.2004.03.001.

Demirel, B., Daver, F., 2009. The effects on the properties of PET bottles of changes to bottle-base geometry. J. Appl. Polym. Sci. 114, 3811–3818. https://doi.org/10.1002/app.30990.

Doumeng, M., Makhlouf, L., Berthet, F., Marsan, O., Delbé, K., Denape, J., Chabert, F., 2021. A comparative study of the crystallinity of polyetheretherketone by using density, DSC, XRD, and Raman spectroscopy techniques. Polym. Test. 93, 106878 https://doi.org/10.1016/j.polymertesting.2020.106878.

Eriksen, M.K., Christiansen, J.D., Daugaard, A.E., Astrup, T.F., 2019. Closing the loop for PET, PE and PP waste from households: Influence of material properties and product design for plastic recycling. Waste Manag. 96, 75–85. https://doi.org/10.1016/J.WASMAN.2019.07.005.

Evans, R.J., Milne, T.A., 1987. Molecular characterization of the pyrolysis of biomass. Energy Fuels 1, 123–137. https://doi.org/10.1021/ef00002a001.

Fuentes-Cano, D., Gómez-Barea, A., Nilsson, S., 2013. Generation and secondary conversion of volatiles during devolatilization of dried sewage sludge in a fluidized bed. Undefined 52, 1234–1243. https://doi.org/10.1021/IE302678U.

Fuentes-Cano, D., Gómez-Barea, A., Nilsson, S., Ollero, P., 2016. Kinetic modeling of tar and light hydrocarbons during the thermal conversion of biomass. Energy Fuels 30, 377–385. https://doi.org/10.1021/acs.energyfuels.5b02131.

Gojny, F.H., Schulte, K., 2004. Functionalisation effect on the thermo-mechanical behaviour of multi-wall carbon nanotube/epoxy-composites. Compos. Sci. Technol. 64, 2303–2308. https://doi.org/10.1016/j.compscitech.2004.01.024.

Gürel, K., Magalhães, D., Kazanç, F., 2022. The effect of torrefaction, slow, and fast pyrolysis on the single particle combustion of agricultural biomass and lignite coal at high heating rates. Fuel 308, 122054. https://doi.org/10.1016/j.fuel.2021.122054.

Hakeem, I.G., Aberuagba, F., Musa, U., 2018. Catalytic pyrolysis of waste polypropylene using Ahoko kaolin from Nigeria. Appl. Petrochem. Res 8, 203–210. https://doi.org/10.1007/s13203-018-0207-8.

Hayashi, J., Nakagawa, K., Kusakabe, K., Morooka, S., Yumura, M., 1992. Change in molecular structure of flash pyrolysis tar by secondary reaction in a fluidized bed reactor. Fuel Process. Technol. 30, 237–248. https://doi.org/10.1016/0378-3820(92)90052-R.

Hsu, C.J., Tu, C.W., Huang, Y.W., Kuo, S.W., Lee, R.H., Liu, Y.T., Hsueh, H.Y., Aimi, J., Huang, C.F., 2021. Synthesis of poly(styrene)-b-poly(2-vinyl pyridine) four-arm star block copolymers via ATRP and their self-assembly behaviors. Polym. (Guildf.) 213, 123212. https://doi.org/10.1016/j.polymer.2020.123212.

Jess, A., 1996. Mechanisms and kinetics of thermal reactions of aromatic hydrocarbons from pyrolysis of solid fuels. Fuel 75, 1441–1448. https://doi.org/10.1016/0016-2361(96)00136-6.

Kaminsky, W., 2021. Chemical recycling of plastics by fluidized bed pyrolysis. Fuel Commun. 8, 100023 https://doi.org/10.1016/J.JFUECO.2021.100023.

Kato, L.S., Conte-Junior, C.A., 2021. Safety of plastic food packaging: the challenges about non-intentionally added substances (NIAS) discovery, identification and risk assessment. Polym. (Basel) 13, 2077. https://doi.org/10.3390/polym13132077.

Kenny, S.T., Runic, J.N., Kaminsky, W., Woods, T., Babu, R.P., Keely, C.M., Blau, W., O'Connor, K.E., 2008. Up-cycling of PET (polyethylene terephthalate) to the biodegradable plastic PHA (polyhydroxyalkanoate. Environ. Sci. Technol. 42, 7696–7701. https://doi.org/10.1021/ES801010E.

Kim, K.J., Doi, Y., Abe, H., 2006. Effects of residual metal compounds and chain-end structure on thermal degradation of poly(3-hydroxybutyric acid. Polym. Degrad. Stab. 91, 769–777. https://doi.org/10.1016/J.POLYMDEGRADSTAB.2005.06.004.

Lefeuvre, et al., 2017. Anticipating in-use stocks of carbon fiber reinforced polymers and related waste flows generated by the commercial aeronautical sector until 2050. Resour. Conserv. Recycl. 125 (2017), 264–272.

Lefeuvre A., Garnier S., Jacquemin, L. and et al. (2019) Anticipating in-use stocks of carbon fibre reinforced polymers and related waste generated by the wind power sector until 2050.

Li, H., Englund, K., 2017. Recycling of carbon fiber-reinforced thermoplastic composite wastes from the aerospace industry. J. Compos. Mater. 51, 1265–1273. https://doi.org/10.1177/0021998316671796.

Li, J., Yang, Y., Xiao, Y., Tang, B., Ji, Y., Liu, S., 2021. Glucose-derived carbon nanospheres as flame retardant for polyethylene terephthalate. Front. Mater. 8. https://doi.org/10.3389/fmats.2021.790911.

Li, Y.F., Li, J.Y., Ramanathan, G.K., Chang, S.M., Shen, M.Y., Tsai, Y.K., Huang, C.H., 2021. An experimental study on mechanical behaviors of carbon fiber and microwave-assisted pyrolysis recycled carbon fiber-reinforced concrete. Sustain 13, 6829. https://doi.org/10.3390/su13126829.

Lu, C., Xu, N., Zheng, T., Zhang, X., Lv, H., Lu, X., Xiao, L., Zhang, D., 2019. The optimization of process parameters and characterization of high-performance CF/PEEK composites prepared by flexible CF/PEEK plain weave fabrics. Polymers (Basel) 11, 53. https://doi.org/10.3390/polym11010053.

Maafa, I.M., 2021. Pyrolysis of polystyrene waste: aa review. Polymers (Basel) 13, 1–30. https://doi.org/10.3390/polym13020225.

Magalhães, D., Gürel, K., Matsakas, L., Christakopoulos, P., Pisano, I., Leahy, J.J., Kazanç, F., Trubetskaya, A., 2021. Prediction of yields and composition of char from fast pyrolysis of commercial lignocellulosic materials, organosolv fractionated and torrefied olive stones. Fuel 289, 119862. https://doi.org/10.1016/j.fuel.2020.119862.

Maqsood, et al., 2021. Pyrolysis of plastic species: A review of resources and products. J. Anal. Appl. Pyrolysis 159, 105295.

Meyer, L.O., Schulte, K., Grove-Nielsen, E., 2009. CFRP-recycling following a pyrolysis route: process optimization and potentials. J. Compos. Mater. 1121–1132. https://doi.org/10.1177/0021998308097737.

Miao, Y., von Jouanne, A., Yokochi, A., 2021. Current technologies in depolymerization process and the road ahead. Polymers (Basel) 13, 1–17. https://doi.org/10.3390/polym13030449.

Modi, S., Koelling, K., Vodovotz, Y., 2011. Assessment of PHB with varying hydroxyvalerate content for potential packaging applications. Eur. Polym. J. 47, 179–186. https://doi.org/10.1016/j.eurpolymj.2010.11.010.

Narancic, T., Cerrone, F., Beagan, N., O'Connor, K.E., 2020. Recent advances in bioplastics: application and biodegradation. Polymers (Basel) 12, 920. https://doi.org/10.3390/POLYM12040920.

Naser, A.Z., Deiab, I., Defersha, F., Yang, S., 2021. Expanding poly(lactic acid) (PLA) and polyhydroxyalkanoates (PHAs) applications: a review on modifications and effects. Polymers (Basel) 13, 4271. https://doi.org/10.3390/polym13234271.

Nguyen, H.T.H., Qi, P., Rostagno, M., Feteha, A., Miller, S.A., 2018. The quest for high glass transition temperature bioplastics. J. Mater. Chem. A 6, 9298–9331. https://doi.org/10.1039/c8ta00377g.

Obruca, S., Benesova, P., Petrik, S., Oborna, J., Prikryl, R., Marova, I., 2014. Production of polyhydroxyalkanoates using hydrolysate of spent coffee grounds. Process Biochem 49, 1409–1414. https://doi.org/10.1016/j.procbio.2014.05.013.

Ogunkanmi, J.O., Kulla, D.M., Omisanya, N.O., Sumaila, M., Obada, D.O., Dodoo-Arhin, D., 2018. Extraction of bio-oil during pyrolysis of locally sourced palm kernel shells: effect of process parameters. Case Stud. Therm. Eng. 12, 711–716. https://doi.org/10.1016/j.csite.2018.09.003.

Oliveux, G., Dandy, L.O., Leeke, G.A., 2015. Current status of recycling of fibre reinforced polymers: review of technologies, reuse and resulting properties. Prog. Mater. Sci. https://doi.org/10.1016/j.pmatsci.2015.01.004.

Pacheco-López, A., Lechtenberg, F., Somoza-Tornos, A., Graells, M., Espuña, A., 2021. Economic and environmental assessment of plastic waste pyrolysis products and

biofuels as substitutes for fossil-based fuels. Front. Energy Res. 9. https://doi.org/10.3389/fenrg.2021.676233.
Pakdel, E., Kashi, S., Varley, R., Wang, X., 2021. Recent progress in recycling carbon fibre reinforced composites and dry carbon fibre wastes. Resour. Conserv. Recycl. https://doi.org/10.1016/j.resconrec.2020.105340.
Palmeiro-Sánchez, T., Graham, A., Lens, P.N.L., O'Flaherty, V., 2022. Temperature influence in the biosynthesis of polyhydroxyalkanoates by mixed microbial cultures – systems' performance and biopolymer properties. SSRN Electron. J. https://doi.org/10.2139/ssrn.4051098.
Palmeiro-Sánchez, T., Val Del Rio, A., Fra-Vázquez, A., Luis Campos, J., Mosquera-Corral, A., 2019. High-yield synthesis of poly(3-hydroxybutyrate-co-3-hydroxyvalerate) copolymers in a mixed microbial culture: effect of substrate switching and F/M ratio. Ind. Eng. Chem. Res. 58, 21921–21926. https://doi.org/10.1021/ACS.IECR.9B03514.
Papari, S., Bamdad, H., Berruti, F., 2021. Pyrolytic conversion of plastic waste to value-added products and fuels: a review. Materials (Basel) 14, 2586. https://doi.org/10.3390/ma14102586.
Pei, L., Schmidt, M., Wei, W., 2011. Conversion of biomass into bioplastics and their potential environmental impacts. Biotechnol. Biopolym. https://doi.org/10.5772/18042.
Polman, E.M.N., Gruter, G.J.M., Parsons, J.R., Tietema, A., 2021. Comparison of the aerobic biodegradation of biopolymers and the corresponding bioplastics: a review. Sci. Total Environ. 753, 141953 https://doi.org/10.1016/j.scitotenv.2020.141953.
RameshKumar, S., Shaiju, P., O'Connor, K.E., P, R.B., 2020. Bio-based and biodegradable polymers - state-of-the-art, challenges and emerging trends. Curr. Opin. Green. Sustain. Chem. 21, 75–81. https://doi.org/10.1016/j.cogsc.2019.12.005.
Raza, Z.A., Riaz, S., Banat, I.M., 2018. Polyhydroxyalkanoates: properties and chemical modification approaches for their functionalization. Biotechnol. Prog. 34, 29–41. https://doi.org/10.1002/btpr.2565.
Rudin, A., Choi, P., 2013. Biopolymers. Elem. Polym. Sci. Eng. 521–535. https://doi.org/10.1016/B978-0-12-382178-2.00013-4.
Saha, B., Ghoshal, A.K., 2006. Model-fitting methods for evaluation of the kinetics triplet during thermal decomposition of poly(ethylene terephthalate) (PET) soft drink bottles. Ind. Eng. Chem. Res. 45, 7752–7759. https://doi.org/10.1021/ie060282x.
Sauer M. (2019) Carbon Composites e.V. Composites-Marktbericht.
Schrader, J.A., McCabe, K.G., Srinivasan, G., Haubrich, K., Grewell, D., Madbouly, S., Graves, W.R., 2015. Development and evaluation of bioplastic containers for sustainable greenhouse and nursery production. Acta Hortic. 1104, 79–88. https://doi.org/10.17660/ActaHortic.2015.1104.13.
Seiler, E., Teipel, U., 2018. Recycling von polymeren Verbundstrukturen aus Rotorblättern. In: Recycling and Rohstoffe Bd. 11. TK Verlag GmbH, Neuruppin.
Serenko, O.A., Roldughin, V.I., Askadskii, A.D., Serkova, E.S., Strashnov, P.V., Shifrina, Z.B., 2017. The effect of size and concentration of nanoparticles on the glass transition temperature of polymer nanocomposites. RSC Adv. 7, 50113–50120. https://doi.org/10.1039/c7ra08152a.
Singh, R.K., Ruj, B., Sadhukhan, A.K., Gupta, P., 2019. Thermal degradation of waste plastics under non-sweeping atmosphere: Part 1: effect of temperature, product optimization, and degradation mechanism. J. Environ. Manag. 239, 395–406. https://doi.org/10.1016/j.jenvman.2019.03.067.
Singh, R.K., Ruj, B., Sadhukhan, A.K., Gupta, P., 2020. Thermal degradation of waste plastics under non-sweeping atmosphere: part 2: effect of process temperature on product characteristics and their future applications. J. Environ. Manag. 261, 110112 https://doi.org/10.1016/j.jenvman.2020.110112.
Singh, R.K., Ruj, B., Sadhukhan, A.K., Gupta, P., 2020. A TG-FTIR investigation on the co-pyrolysis of the waste HDPE, PP, PS and PET under high heating conditions. J. Energy Inst. 93, 1020–1035. https://doi.org/10.1016/j.joei.2019.09.003.
Sokoli, H.U., Simonsen, M.E., Søgaard, E.G., 2017. Investigation of degradation products produced by recycling the solvent during chemical degradation of fiber-reinforced composites. J. Reinf. Plast. Compos 36, 1286–1296. https://doi.org/10.1177/0731684417707060.
Stockschläger, J., Quicker, P., Thiel, C., Beckmann, M., Baumann, W., Wexler, M., 2018. Treatment of Carbon Fibre-Containing Waste in Municipal Waste Incineration Plants – Intermediate Results of Practical Studies on an Industrial Scale. In: Mineralische Nebenprodukte und Abfälle 5. TK Verlag GmbH, Neuruppin.
Streitwieser, A., Heathcock, C.H., 1981. Introduction to organic chemistry. Macmillan Publishing, 2nd ed. Macmillan Publishing, New York.
Szacherska, K., Oleskowicz-Popiel, P., Ciesielski, S., Mozejko-Ciesielska, J., 2021. Volatile fatty acids as carbon sources for polyhydroxyalkanoates production. Polymers (Basel) 13, 1–21. https://doi.org/10.3390/polym13030321.
Tang, L.C., Wan, Y.J., Yan, D., Pei, Y.B., Zhao, L., Li, Y.B., Wu, L., Bin, Jiang, J.X., Lai, G. Q., 2013. The effect of graphene dispersion on the mechanical properties of graphene/epoxy composites. Carbon N. Y. 60, 16–27. https://doi.org/10.1016/j.carbon.2013.03.050.
Trubetskaya, A., Souihi, N., Umeki, K., 2019. Categorization of tars from fast pyrolysis of pure lignocellulosic compounds at high temperature. Renew. Energy 141, 751–759. https://doi.org/10.1016/j.renene.2019.04.033.
Trubetskaya, A., Scholten, P.B.V., Corredig, M., 2022. Changes towards more sustainable food packaging legislation and practices. A survey of policy makers and stakeholders in Europe. Food Packag. Shelf Life 32, 100856. https://doi.org/10.1016/J.FPSL.2022.100856.
Trubetskaya, A., Jensen, P.A., Jensen, A.D., Steibel, M., Spliethoff, H., Glarborg, P., 2015. Influence of fast pyrolysis conditions on yield and structural transformation of biomass chars. Fuel Process. Technol. 140, 205–214. https://doi.org/10.1016/j.fuproc.2015.08.034.
Umeki, K., Yamamoto, K., Namioka, T., Yoshikawa, K., 2010. High temperature steam-only gasification of woody biomass. Appl. Energy 87, 791–798. https://doi.org/10.1016/j.apenergy.2009.09.035.
Varshney, S.K., Zhong, X.F., Eisenberg, A., 1993. Anionic homopolymerization and block copolymerization of 4-vinylpyridine and its investigation by high-temperature size-exclusion chromatography in N-methyl-2-pyrrolidinone. Macromolecules 26, 701–706. https://doi.org/10.1021/ma00056a022.
Williams, E.A., Williams, P.T., 1997. Analysis of products derived from the fast pyrolysis of plastic waste. J. Anal. Appl. Pyrolysis 40–41, 347–363. https://doi.org/10.1016/S0165-2370(97)00048-X.
Wolfesberger-Schwabl, U., Aigner, I., Hofbauer, H., 2012. Mechanism of tar generation during fluidized bed gasification and low temperature pyrolysis. Ind. Eng. Chem. Res. 51, 13001–13007. https://doi.org/10.1021/IE300827D.
Yansaneh, O.Y., Zein, S.H., 2022. Recent advances on waste plastic thermal pyrolysis: a critical overview. Processes. https://doi.org/10.3390/pr10020332.